PRAMANA — journal of physics

Vol. 76, No. 4
April 2011
pp. 603–612

Goos–Hänchen shift for higher-order Hermite–Gaussian beams

DHEERAJ GOLLA[1] and S DUTTA GUPTA[2,*]

[1]Indian Institute of Technology Kharagpur, Kharagpur 721 302, India
[2]School of Physics, University of Hyderabad, Hyderabad 500 046, India
*Corresponding author. E-mail: sdghyderabad@gmail.com

MS received 31 July 2010; revised 13 October 2010; accepted 14 October 2010

Abstract. We study the reflection of a Hermite–Gaussian beam at an interface between two dielectric media. We show that unlike Laguerre–Gaussian beams, Hermite–Gaussian beams undergo no significant distortion upon reflection. We report Goos–Hänchen shift for all the spots of a higher-order Hermite–Gaussian beam near the critical angle. The shift is shown to be insignificant away from the critical angle. The calculations are carried out neglecting the longitudinal component along the direction of propagation for a spatially finite, s-polarized, full 3D vector beam. We briefly discuss the difficulties associated with the paraxial approximation pertaining to a vector Gaussian beam.

Keywords. Goos–Hänchen shift; finite beams; total internal reflection; paraxial approximation.

PACS Nos 42.10; 42.25.Gy; 42.25.Bs; 42.30.Kq

1. Introduction

The Goos–Hänchen (GH) shift, first discovered experimentally in 1947, refers to the longitudinal displacement of a beam from its expected geometric position under total internal reflection [1]. Artmann [2] was the first to provide a theoretical explanation of the effect using the stationary phase approximation. A somewhat different calculation of the Goos–Hänchen shift using the conservation of energy was put forth by Renard [3]. Quantitatively the GH shift can be interpreted as the shift of the peak intensity spot of the beam [2] or the weighted mean position of the beam [4]. A thorough theoretical analysis of the effect was carried out by Lotsch [5] in 1968. The effect, although discovered quite a while ago, still remains a topic of interest in current optics literature. The current interest in GH shift is further fueled by several means for enhancing the effect and its use for sensing [6]. These include structures involving absorbing media [7,8], metals [9] and left-handed metamaterials [10,11]. Recent studies focus on systems supporting surface plasmon resonances [6,12,13] and frustrated total internal reflection [14]. From a theoretical angle, most of the studies on GH shift used to suffer from two major drawbacks. First, an overwhelming majority deal with two-dimensional fundamental beams (the third dimension is supressed)

[15–17], and second, they overlook the vector characteristics of the beam. Recall that the paraxial electromagnetic wave is not an exact solution of the Maxwell's equations, but holds only to the first order in $1/k$ (k being the magnitude of the wavevector). Since the pioneering work by Agrawal and Pattanayak [18], the difficulties associated with the paraxial approximation are now clear. The vector nature of the beams adds to the complexity of the problem (leading to a longitudinal field component). Only recently vector Gaussian beams have been dealt within the context of propagation in a uniform medium [19]. A systematic treatment of GH shift for a fundamental vector Gaussian beam was given by Aiello and Woerdman [20]. It was shown by the same authors in a later paper that the suppression of the correction due to the longitudinal component recovers Artman formula for the shift [4]. There has been a great deal of interest in the Laguerre–Gaussian beams and their longitudinal and lateral shifts in view of the angular momentum carried by the beam [21–26]. The longitudinal and transverse shifts for the Laguerre–Gaussian beams were calculated by Bliokh *et al* [24] and verified experimentally by Merano *et al* [25]. Another recent paper presents both theoretical and experimental results on the shift of Laguerre-Gaussian beams and its distortion under reflection and transmission [26]. However, no such studies exist for simpler Hermite–Gaussian beams. In this paper we concentrate on a general vector Hermite–Gaussian beam with s-polarization and look at the reflection of the same from a denser to lighter medium interface. We show how the longitudinal component arises from a simple description of the vector field by means of scalar and vector potentials. Neglecting the longitudinal component under the strong paraxial approximation, we use an angular spectrum decomposition to calculate the reflected field for each spatial harmonic. Summing up the harmonics we end up with the reflected beam profile.

The structure of the paper is as follows. In §2, we provide a simple mathematical formulation of the problem and show that a longitudinal component is inevitable in the paraxial formulation. In §3, we first validate our code by matching our numerical results with those predicted by Artman formula. Next, we present the contour plots for fundamental and higher-order Hermite–Gaussian beam profiles. We also comment on the possibility of splitting of the reflected beam, which has been observed for tightly focussed beams. Finally, we summarize the main results in the conclusion.

2. Mathematical formulation

Consider the electromagnetic wave of frequency ω described by the electric $\mathbf{E}$ and magnetic $\mathbf{B}$ fields in a medium with dielectric constant ϵ and permeability constant $\mu = 1$. Let the scalar and vector potentials be ϕ and $\mathbf{A}$, so that

$$\mathbf{B} = \nabla \times \mathbf{A} = \mathbf{H}, \tag{1}$$

$$\mathbf{E} = -\nabla\phi - \frac{1}{c}\frac{\partial \mathbf{A}}{\partial t} = -\nabla\phi + ik_0\mathbf{A}, \tag{2}$$

where $k_0 = \omega/c$ is the vacuum wave vector. Under the Lorentz condition, the vector $\mathbf{A}$ satisfies the following equations:

$$\nabla \cdot \mathbf{A} - ik_0\epsilon\phi = 0, \tag{3}$$

$$\nabla^2\mathbf{A} + k_0^2\epsilon\mathbf{A} = 0. \tag{4}$$

One way to tackle the problem is to ignore the variation of all quantities in one direction, making it effectively a two-dimensional problem. Polarization is no longer an issue in the two-dimensional scenario and the standard scalar approximation techniques can be used. A more general set of solutions is obtained by assuming that vector **A**, rather than **E** is polarized in a particular direction.

We seek the solution of **A** in the form of a wave propagating along $\hat{\mathbf{z}}$ with transverse polarization (say along $\hat{\mathbf{x}}$). Such a solution takes the form

$$\mathbf{A} = [a(x, y, z)\mathrm{e}^{ikz} + \mathrm{cc}\hat{\mathbf{x}}, \tag{5}$$

where $k = k_0\sqrt{\epsilon}$ and $a(x, y, z)$ is the slowly varying (with respect to z) amplitude. Using eqs (3) and (5), $\nabla\phi$ can be evaluated to be

$$\nabla\phi = (ik_0\epsilon)^{-1}\nabla\left(\frac{\partial a}{\partial x}\exp(ikz)\right), \tag{6}$$

which subsequently leads to the expression of **E** as follows:

$$\mathbf{E} = ik_0\left(a\hat{\mathbf{x}} + \frac{i}{k}\frac{\partial a}{\partial x}\hat{\mathbf{z}}\right)\exp(ikz). \tag{7}$$

It is clear from eq. (7) that the paraxial approximation inevitably leads to a longitudinal component. Substituting expression (5) in eq. (4) and making use of the slowly varying approximation one can write down the paraxial equation for a light beam:

$$\frac{\partial^2 a}{\partial x^2} + \frac{\partial^2 a}{\partial y^2} + 2ik\frac{\partial a}{\partial z} = 0. \tag{8}$$

The solution of eq. (8) can be expressed as

$$a(x, y, z) = \int \tilde{a}(q_x, q_y)\exp[i(q_x x + q_y y)]\exp\left(-i\left(\frac{{q_x}^2 + {q_y}^2}{2k^2}\right)z\right)\mathrm{d}q_x\mathrm{d}q_y. \tag{9}$$

For localized profiles of the form $\tilde{a}(q_x, q_y)$, one has solutions in the form of a beam. For example, for

$$\tilde{a}(q_x, q_y) = \pi {W_0}^2\exp\left(-{W_0}^2\left(\frac{{q_x}^2 + {q_y}^2}{4}\right)\right), \tag{10}$$

one recovers the fundamental Gaussian beam

$$a(x, y, z) = \frac{W_0}{W(z)}\exp\left(\frac{-r^2}{W^2(z)}\right)\exp\left(\frac{ikr^2}{2R(z)}\right)\exp(-i\varphi(z))\exp(ikz). \tag{11}$$

The expressions for the beam waist $W(z)$, radius of curvature $R(z)$ and Gouy phase $\varphi(z)$ in the above expression are standard. Following a similar route, the expression for the general Hermite–Gaussian beam can be calculated. To calculate the reflected beam profiles

for higher-order Hermite–Gaussian modes, we have taken the incident beam amplitude as follows:

$$a_{m,n} = \frac{W_0}{W(z)} \exp\left(\frac{-r^2}{W^2(z)}\right) \exp\left(\frac{ikr^2}{2R(z)}\right) \exp\left(-i\varphi(z)_{m,n}\right) \times \exp(ikz) H_m\left(\frac{\sqrt{2}x}{W(z)}\right) H_n\left(\frac{\sqrt{2}y}{W(z)}\right), \tag{12}$$

where $W(z)$ and $R(z)$ have the same meaning as before, but the Guoy phase takes on the definition

$$\varphi_{m,n}(z) = (m + n + 1) \tan^{-1}\left(\frac{z}{z_r}\right), \tag{13}$$

where $z_r = kw_0^2/2$.

In the context of the problem of calculating the reflection coefficient, we now specify the geometry. The geometry is akin to that considered by Aiello and Woerdman [4]. We consider an interface (at $z = 0$) between vacuum and a dielectric medium with dielectric constant ϵ. Let the beam be incident at an angle θ to $\hat{z}$ and with vector potential polarized along $\hat{y}$. Let z'-axis also coincide with the direction of propagation of the beam. The primed and unprimed axes are oriented at θ to each other. The relation between the unprimed and primed coordinates are given by

$$x' = x\cos\theta - z\sin\theta, \quad y' = y, \quad z' = z\cos\theta + x\sin\theta. \tag{14}$$

For a fundamental Gaussian beam of the form given by eq. (10), **E** reads as follows:

$$\mathbf{E} = \int \left(\hat{\mathbf{y}}' - \frac{q_y'}{k}\hat{\mathbf{z}}'\right) \tilde{a}(q_x', q_y') \times \exp\left[i\left(q_x' x' + q_y' y' - \frac{q_x'^2 + q_y'^2}{2k^2} z' + kz'\right)\right] \mathrm{d}^2 q'. \tag{15}$$

This expression is consistent with the result of Chen *et al* [19], that the choice of a zero transverse field component at the input boundary plane ensures vanishing of the component throughout the propagation in the same medium. The consistency of the magnitude of the total wave vector of every spatial component under the paraxial approximation $\sqrt{{q_x}^2 + {q_y}^2} \ll k$ can easily be verified.

$$q_x'^2 + q_y'^2 + k^2\left(1 - \frac{q_x'^2 + q_y'^2}{2k^2}\right)^2 \approx k^2. \tag{16}$$

Note also that under very weak transverse variation of the field when the inequality $\frac{q_y'}{k}$ ($\ll 1$) holds, eq. (15) leads to a simple s-polarized beam all throughout [26]. Hereafter, we refer to this approximation as the strong paraxial approximation.

Moving to the unprimed coordinate system one can write down a typical plane-wave component of **E** as

$$(e_i{}^x\hat{\mathbf{x}} + e_i{}^y\hat{\mathbf{y}} + e_i{}^z\hat{\mathbf{z}})\tilde{a}(q_x, q_y) \exp[i(q_x x + q_y y + q_z z)], \tag{17}$$

where ${e_i}^x = (-q'_y/k)\sin\theta$, ${e_i}^y = 1$, ${e_i}^z = (-q'_y/k)\cos\theta$ and q_x, q_y and q_z are given by

$$\begin{aligned} q_x &= q'_x\cos\theta + k\sin\theta\left(1 - \frac{q_x'^2 + q_y'^2}{2k^2}\right), \\ q_y &= q'_y, \\ q_z &= q'_x\sin\theta - k\cos\theta\left(1 - \frac{q_x'^2 + q_y'^2}{2k^2}\right). \end{aligned} \tag{18}$$

It is now easy to check the consistency of the total wave vector for a spatial component under the paraxial approximation using the above equations

$${q_x}^2 + {q_y}^2 + {q_z}^2 \approx k^2. \tag{19}$$

In the following discussion, we neglect the terms proportional to q/k in the amplitude, while retaining the full dependence in the phase factors. Thus the beam reduces to an s-polarized beam with only nonvanishing component along $\hat{\mathbf{y}}$. Then, one can easily calculate the reflected component by multiplying the amplitude of the spectral component with the reflection coefficient r_s which is given by

$$r_s = \frac{1 - (q_{z_0}/q_z)}{1 + (q_{z_0}/q_z)}, \tag{20}$$

where $q_{z_0} = \sqrt{k_0^2 - ({q_x}^2 + {q_y}^2)}$. To validate the above approximation, one has to have a broad beam (close to plane-wave profile), so that $\left(q_x'^2 + q_y'^2\right)/k^2 \ll 1$. The broader the beam, the smaller is the GH effect. Note that plane waves do not exhibit any GH shift. Thus one has to exercise care in choosing the parameter domain where the shift, albeit small, is still observable, if one wants to describe the phenomenon with a model of an incident Gaussian beam with a given polarization. For a tightly focussed beam, the paraxial approximation forces one to include the longitudinal component. With the longitudinal component present, the calculation of the reflection and transmission coefficients poses a formidable problem.

3. Numerical results and discussions

In this section we follow the procedure detailed in §2 to calculate the beam profile on the interface before and after the reflection. To be specific, we take a beam described by a scalar function with s-polarization. We find the 2D Fourier components incorporating the oblique incidence. Each Fourier component is multiplied by the corresponding reflection coefficient. Then an inverse Fourier transform leads to the reflected beam profile at $z = 0$. We have considered the cases of fundamental and higher-order Gaussian beams. We show that identity of the beam is retained for Hermite–Gaussian beams. In all our calculations we have taken $\sqrt{\epsilon} = 1.7321$ (the medium of incidence), $\epsilon_0 = 1.0$ and $kW_0 = 40$, unless specified otherwise. The incident beam is assumed to be focussed at $z = 0$ (at the interface).

While choosing the relevant parameters, special attention was given to two aspects. First, the sampling frequency was taken to be more than the Nyquist rate [27]. Second, the parameter domain was chosen such that the strong paraxial approximation was valid. For an angle of incidence of $\theta = 40^\circ$ and $kW_0 = 40$, for the y direction, we take the sampling interval to be $\Delta y/W_0 = 0.1020$. Sampling is done inside a square area of side of 15 units. In the inverse Fourier space, the sampling interval is $\Delta q_y = 0.0602$. Let $\widetilde{q_y}$ represents the value at which the amplitude falls off, say, 10^{-5} times the peak value. The value of $\widetilde{q_y}$ gives an estimate of the angular dispersion of the incident beam. For a fundamental Gaussian beam with $kW_0 = 40$, we have $\widetilde{q_y} \approx 0.17$. Thus the chosen parameters alleviate both the above concerns.

We first use the numerical method to predict the GH shift for a two-dimensional Gaussian beam. Figure 1 shows the dependence of the GH shift (normalized to the beam waist W_0) on the angle of incidence θ for a 2D fundamental Gaussian beam. The GH shift values computed using the procedure described in the previous section (solid line) are contrasted with those predicted by the Artmann formula [15] (dashed line). It is clear from figure 1 that for angles larger than the critical angle and away from it, the GH shift computed numerically falls off and compares well with that predicted by the Artmann formula. Near the critical angle, it is well known that the Artmann formula has a singularity [28]. Thus the stationary phase approximation, which is used to derive the Artmann formula, is not applicable near the critical angle. Our numerical results are consistent with the fact that the GH shift must show a smooth, continuous and finite variation near the critical angle [28].

Having validated our numerical procedure in the two-dimensional case, we now use it to analyse three-dimensional Gaussian beams. The profiles on the interface for the incident and reflected fundamental Gaussian beams are shown in figure 2. The left (right) pane in each horizontal line shows the contour of the incident (reflected) beam at the interface. Horizontal (vertical) axis is the normalized $x(y)$ direction. It is clear from figure 2 that for small and large angles of incidence, away from the critical angle, the shift of the fundamental Gaussian beam is small. Close to the critical angle $\theta_{\rm cr}$ (= $\arcsin(\sqrt{\epsilon_0/\epsilon})$), the shift

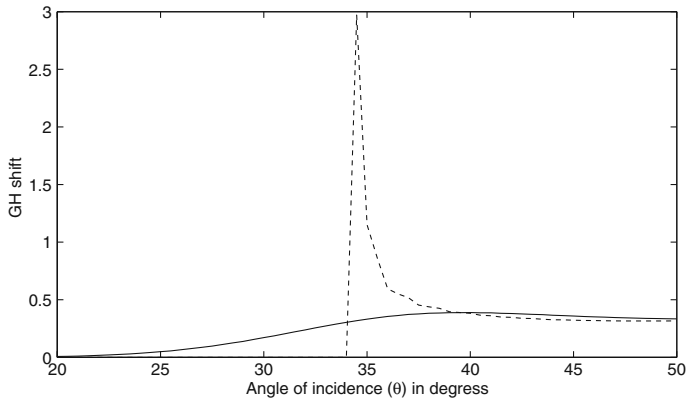

Figure 1. Normalized GH shift as a function of angle of incidence θ. Numerically computed GH shift (solid line) and shift predicted from the Artmann formula (dashed line) are shown.

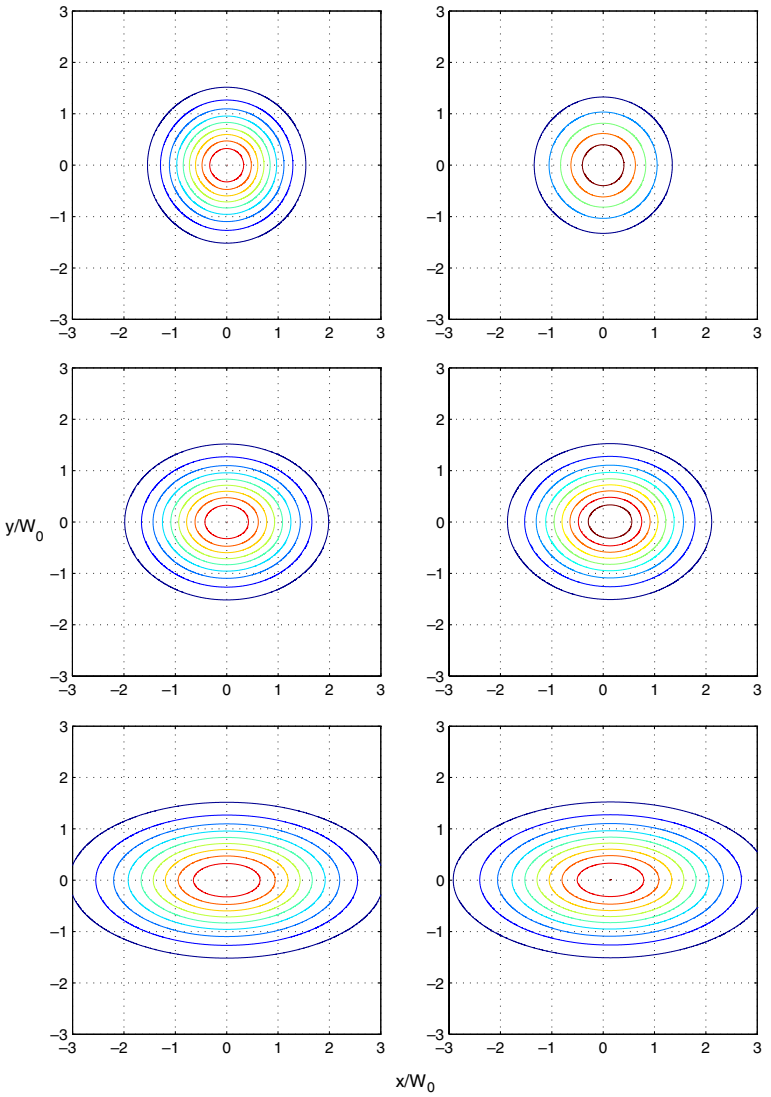

Figure 2. Incident (left) and reflected (right) profiles for fundamental Gaussian beams. The angles of incidence are: 10° (top), 40° (middle), 60° (bottom).

is discernible. Slightly above the critical angle, the shift achieves the maximum value. The GH shift for near normal incidence is almost negligible.

Figure 3 shows the results for TEM_{11} beam incident at 40° (approximately where the GH shift is the largest). It is clear from figure 3 that even after reflection the beam identity of the TEM beam is intact, though there is a slight difference in the heights of the pair of lobes. The shift is smaller away from the critical angle as in the case of the fundamental

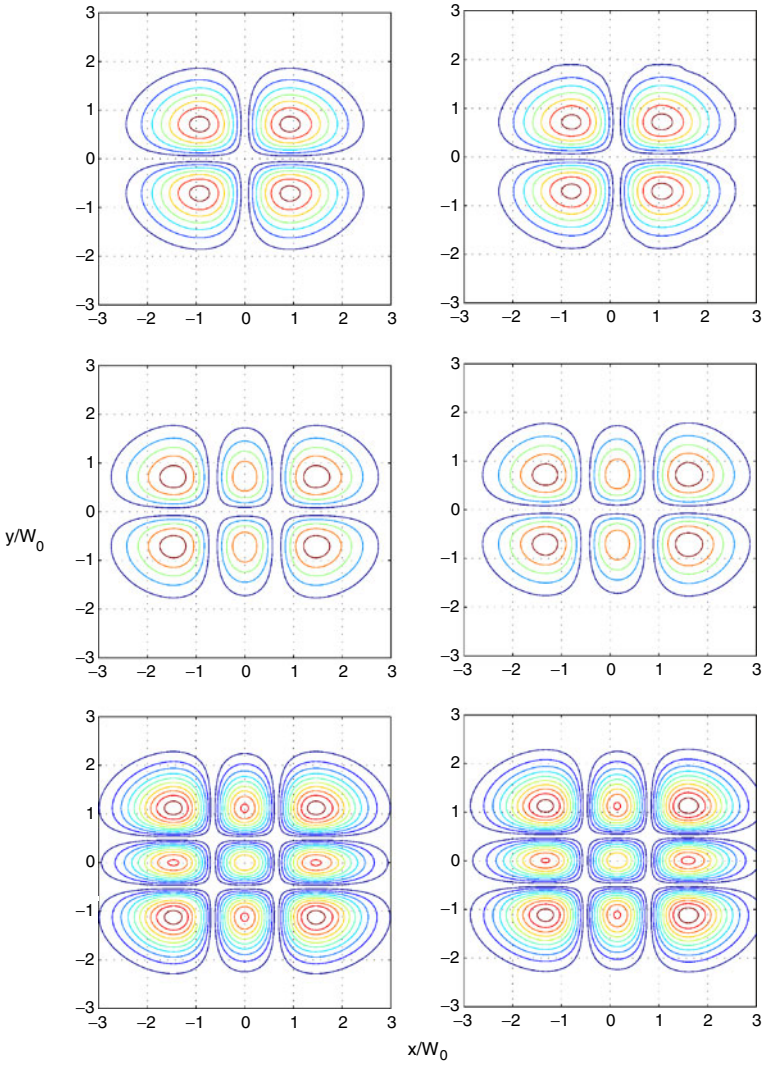

Figure 3. Incident (left) and reflected (right) beam profiles for TEM_{11} (top), TEM_{21} (middle), TEM_{22} (bottom), incident at 40°.

Gaussian beam. Figure 3 also shows the incident and reflected profiles for TEM_{21} (middle) and TEM_{22} (bottom) cases, respectively.

We now focus our attention to beam distortion under reflection near the critical angle. For loosely focussed beams, it was shown that the distortion is negligible for Hermite–Gaussian beams. This is not true for Laguerre–Gaussian beams because of the angular momentum carried by the beam. The inherent orbital angular momentum [22] of the beam and the lateral Feodorov–Imbert shift are responsible for the distortion of the beam profile upon reflection [24,26]. Thus, loosely focussed higher-order Hermite–Gaussian beams can

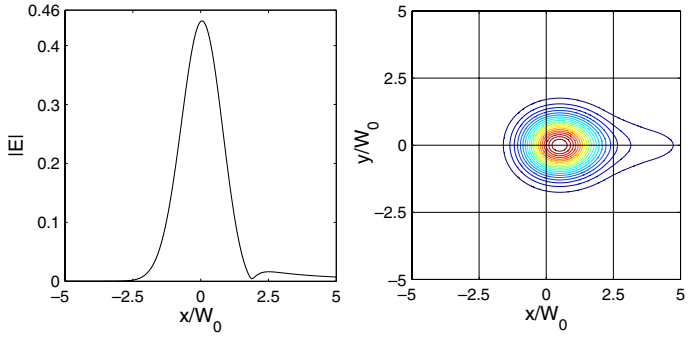

Figure 4. The reflected beam profile for 2D (left) and 3D (right) Gaussian beam incident at 25°.

retain their identity upon reflection, while the Laguerre–Gaussian beams can be distorted beyond recognition.

Until now, we have been looking at broad (loosely focussed) beams which fall well within the realm of validity of the paraxial approximation. We now look at tightly focussed beams which fall at the periphery of this regime. We qualitatively describe the effects of reflection on a tight Gaussian beam. Figure 4 shows the incident and reflected profiles for a tightly focussed ($kW_0 = 15$) fundamental beam for 2D and 3D simulations (left and right panels, respectively). The reflected profile shows a splitting in the beam, with the newly developed lobe having very little intensity compared to the main lobe. This observation is in line with other investigations of a similar kind where beam splitting upon reflection has been reported [13,29]. It has to be kept in mind that very tight beams, by default, fall in the regime of nonparaxial beams and that in this regime the longitudinal component cannot be summarily neglected.

4. Conclusion

In conclusion, we studied the reflection of Gaussian beams from a dielectric–vacuum interface and showed that for tight beams it is advisable to take into account the longitudinal component of the field under paraxial approximation, while one can use standard scalar beams with a given polarization in the opposite case. We numerically studied the reflected beam profiles and demonstrated the GH shift for fundamental and higher-order Gaussian beams. Calculations were carried out after neglecting the longitudinal component of the electric field, which is justified in the strong paraxial approximation regime. We also concluded that higher-order Hermite–Gaussian beams retain their identity after reflection unlike Laguerre–Gaussian beams. For tight beams it is indicative that beam splitting occurs upon reflection, but for more precise results the longitudinal component must be retained in this case. Further investigation is needed to tackle the problem of reflection and associated GH shift of vector beams without making the strong paraxial approximation. Work is underway on enhancing the GH shift of higher-order Gaussian beams using various layered media with metal–dielectric structures and metamaterials.

Acknowledgements

One of the authors (SDG) is thankful to Girish Agarwal for many helpful discussions. The authors are also thankful to Dr Subimal Deb for discussions and help in preparing the manuscript. This work was supported by a grant from the Department of Science and Technology, Government of India.

References

[1] F Goos and H Hanchen, *Ann. Phys.* **1**, 333 (1947)
[2] K Artmann, *Ann. Phys.* **2**, 87 (1948)
[3] R H Renard, *J. Opt. Soc. Am.* **54**, 1190 (1964)
[4] A Aiello and J P Woerdman, *Opt. Lett.* **33**, 1437 (2008)
[5] H Lotsch, *J. Opt. Soc. Am.* **58**, 551 (1968)
[6] X Yin and L Hesselink, *Appl. Phys. Lett.* **89**, 261108 (2006)
[7] W Wild, *Phys. Rev.* **A25**, 2099 (1982)
[8] Yan Wang *et al, J. Opt. Soc. Am.* **A** 105701 (2009)
[9] M Merano *et al*, *Opt. Exp.* **15**, 15928 (2007)
[10] I V Shadrivov *et al, Appl. Phys. Lett.* **83**, 2713 (2003)
[11] De-Kui Qing, *Opt. Exp.* **29**, 872 (2004)
[12] X B Yin *et al*, *Appl. Phys. Lett.* **89**, 261108 (2006)
[13] L Chen *et al*, *J. Opt.* **12**, 075002 (2010)
[14] A Haibel *et al*, *Phys. Rev*. **E63**, 047601 (2001)
[15] M McGuirk and C K Carniglia, *J. Opt. Soc. Am.* **67**, 103 (1977)
[16] K W Chiu and J J Chin, *Am. J. Phys.* **40**, 1847 (1972)
[17] R P Riesz and R Simon, *J. Opt. Soc. Am.* **A2**, 1809 (1985)
[18] G P Agrawal and D N Pattanayak, *J. Opt. Soc. Am.* **69**, 575 (1979)
[19] C G Chen *et al*, *J. Opt. Soc. Am.* **A19**, 404 (2002)
[20] A Aiello and J P Woerdman, arXiv:0710.1643v2 [physics.optics]
[21] S M Barnett and L Allen, *Opt. Comm.* **110**, 670 (1994)
[22] L Allen *et al*, *Phys. Rev.* **A45**, 8185 (1992)
[23] N B Simpson *et al*, *Opt. Lett.* **22**, 52 (1997)
[24] K Y Bliokh *et al*, *Opt. Lett.* **34**, 389 (2009)
[25] M Merano *et al*, *Phys. Rev*. **A82**, 023817 (2010)
[26] H Okuda and H Sasada, *J. Opt. Soc. Am.* **A25**, 881 (2008)
[27] J W Goodman, *Introduction to Fourier optics,* 2nd Edn (McGraw Hill Companies, New York, 1996)
[28] H M Lai *et al*, *J. Opt. Soc. Am.* **A3**, 550 (1986)
[29] Y Wan *et al*, *Opt. Exp.* **17**, 21313 (2009)